JOURNAL OF AEROSPACE SOCIETY MALAYSIA

ARTICLE

BIOMIMETIC MICROSPIKE ENHANCEMENT OF H-ROTOR DARRIEUS WIND TURBINE PERFORMANCE: AN EXPERIMENTAL INVESTIGATION

Nur Faraihan Zulkefli [1,*], Muhammad Saiful Izzat Hisham [1] and Nurhayati Mohd Nur [1]

1. Aerospace Research Centre, Aerospace Department, Universiti Kuala Lumpur-Malaysian Institute of Aviation Technology, Dengkil, Selangor, Malaysia.

*Correspondence: nurfaraihan@unikl.edu.my

Abstract: The H-Rotor Darrieus vertical-axis wind turbine (VAWT) offers advantages for distributed energy generation but it unfortunately also suffers from poor low-wind-speed performances due to its aerodynamic inefficiency. On the other hand, there is an opportunity to apply biomimetic flow control strategies that have been inspired by the natural systems for passive performance enhancement without mechanical complexity. Taking this into account, this study investigates the application of the dragonfly-inspired microspikes to the turbine blades of a H-Rotor Darrieus wind turbine. In this study, the small-scale prototype H-Rotor Darrieus wind turbine with NACA 4415 airfoil blades has been designed and fabricated using additive manufacturing process. The microspikes are positioned at 30% chord from the leading edge of the blades to generate boundary layer vortices. The resultant performance effect of the microspikes is tested outdoor with uncontrolled environment and compared with baseline blades. Overall, the results have demonstrated an increase of approximately 18.5% in blade rotation, 22% in torque coefficient, 18.7% in tip speed ratio and also almost 0.5% in both wind power and power output. This is taken to show that the blades with microspike vortex generators have the potential to re-energize the boundary layer, delay flow separation and significantly increase lift and reduce drag. Furthermore, the power output capacity and aerodynamic efficiency of the H-Rotor Darrieus wind turbine are shown to significantly increase with the microspike vortex generators attached to its airfoil blades.

Keywords: dragonfly inspired, H-Rotor Darrieus, microspike, renewable energy, vertical-axis wind turbine

1. Introduction

Nowadays, wind energy plays a major role in the global clean energy transition, mainly dominated by large multi-megawatt wind farms. However, there is a growing shift toward small-scale wind energy systems for the urban and residential applications. The vertical-axis wind turbines (VAWTs) are gaining attention due to their easier integration, although they also have a lower performance compared to the horizontal-axis wind turbines (HAWTs) [1]. Unlike HAWTs, VAWTs capture the wind energy from any direction without requiring yaw mechanisms, making it suitable for turbulent, multi-directional wind regimes that are typical of the built environment [2]. Among the VAWT designs, the Darrieus turbine represents a lift-based configuration that offers a higher theoretical efficiency than drag-based designs. The H-Rotor variant, featuring straight vertical blades mounted on a central shaft, has attracted renewed interest due to its structural simplicity of power coefficient compared to curve-blade configurations [3]. It is noted that the manufacturing process of straight blades is considerably less complex than producing curved geometries, reducing fabrication costs and enabling standardized production methods. Recent

market analyses have shown a growing demand for small-scale wind turbines in the range of 1 kW to 10 kW for residential and commercial applications, where the H-Rotor designs can compete effectively with solar photovoltaics in moderate-to-high wind resource areas [4]. However, the H-Rotor Darrieus turbines still face aerodynamic problems that limit their use. The main issues for the H-Rotor Darrieus wind turbine are its poor performance at low wind speeds and its self-starting difficulty in normal wind conditions [5]-[6]. As the blades rotate, the angle of attack also changes constantly, causing unsteady airflow. When the blade moves downstream, flow separation occurs on the suction side, which reduces lift and also increases drag. This subsequently will lower the efficiency and make it harder for the wind turbine to start on its own. The conventional H-Rotor Darrieus turbines often have a power coefficient between 0.25 and 0.35 [7]-[8], which is lower than the Betz limit of 0.59. In comparison, the modern HAWTs have a power coefficient in the range between 0.45 to 0.50. Furthermore, H-Rotor Darrieus wind turbine reaches its efficiency only in a small range of tip speed ratio, therefore its performance is limited. At wind speed below 5 m/s, many H-Rotor Darrieus wind turbines are unable to produce the adequate power, making them less suitable for areas with moderate wind resources.

To overcome these limitations, numerous modifications have been proposed to improve H-Rotor Darrieus turbines. These approaches generally fall into three primary categories: blade shape (geometric modification), addition of auxiliary devices and use of flow control techniques to enhance aerodynamic efficiency. In general, geometry modification focusses on altering the shape of the blade to improve its aerodynamic characteristics. Recent works include the investigation by Korukcu [2], who used dimpled blade surface to create localized flow disturbance that delays the separation. The result demonstrated that the power coefficient is improved by 5% to 7% through strategic dimple placement. Additionally, Eltayesh et al. [1] have shown that the addition of dimples also can provide a stable performance across a range of wind situations. Moreover, curve and swept blade designs, inspired by biological forms, have achieved improvement up to 14% by tailoring the spanwise flow characteristics [8]. However, despite the improvement, it is noted that these geometric changes also complicate the manufacturing process and increase structural loads. In the meantime, the auxiliary device strategies involve the employment of additional components to augment the turbine's performance. Auxiliary blades that are strategically positioned around the main rotor have shown promising results. Reddy et al. [3] have reported a power coefficient increment of 22% and a torque improvement of 84% through the optimized auxiliary blade implementation while Asadbeigi et al. [5] have achieved up to 34% enhancement of power coefficient with improved economic viability. Guide vanes represent another auxiliary approach, with Mirmotahari et al. [9] have demonstrated an efficiency improvement up to 55% by using semi-directional airfoil guide vanes. Double deflector systems have achieved even more dramatic gains, with Chen et al. [10] reported 70% higher power coefficient compared to bare rotors. Despite these impressive results, it can be noted that the auxiliary devices add mechanical complexity, increase structural loading and require additional maintenance. Last but not least, flow control mechanisms manipulate the boundary layer or the wake characteristics without major geometric changes. Plain flaps at various chord positions have increased the power coefficient by 19% to 43%, depending on the configuration [7]. In addition, Hosseini Rad et al. [6] have systematically studied vortex cavities and deflectors, demonstrating an increment of power coefficient up to 25% with optimal layouts. Drag-disturbed flow devices improve the startup torque by approximately 42% and the operational torque by 7.5% [4]. High-efficiency vortex structures that are attached to blade surfaces have shown a 34% improvement in power coefficient [11]. The passive flow control approaches are able to offer advantages in simplicity and reliability, although their effectiveness varies considerably with the operating conditions. An identified critical gap in the existing research is the limited exploration of biomimetic surface microstructures for VAWT performance enhancement. While numerous studies have examined the macro-scale modifications and auxiliary devices, only a few have investigated the potential of micro-scale surface features that are inspired by nature.

Due to distinctive wing design, which has evolved over millions of years, dragonflies demonstrate outstanding aerodynamic capability at low Reynolds numbers. The wing's surface of a dragonfly is not

smooth. Instead, it has microspike tubercles and corrugations. The microspikes will mix the slower air speed near the surface with the faster air from above to form tiny vortices that will hold the airflow to the wing and avoid flow separation [12]. As for the effect of lift and drag caused by the microspike on the dragonfly's wing, the drag reduces by almost 3% on the flat plate and the formation of vortices is prevented. This smoother airflow reduces drag and may also contribute to lift improvement [13]. The dragonfly's microspike can be compared to conventional vortex generator on the aircraft's wing, which create many small vortices that efficiently regulate the airflow without causing significant drag. To date, the microspike surface treatments are still mostly unexplored in the wind turbine research despite the obvious biological precedent and compelling scaling arguments. On the other hand, it can be noted that prior researches have mostly ignored the potential of distributed micro-scale features in favor of macro-scale vortex generators or tubercle modifications that are modelled after the flippers of the humpback whales [14]. As microspike features may be easier to incorporate into the current manufacturing process than making significant geometric changes, this oversight presents both a scientific gap and a practical opportunity. This research aims to experimentally investigate aerodynamic performance enhancement of H-Rotor Darrieus VAWT through application of dragonfly-inspired microspike vortex generators. The work in this study involves designing and fabricating microspikes on the NACA 4415 airfoil blades using additive manufacturing, evaluating resultant performance improvement in terms of blade rotation, torque coefficient, tip speed ratio and power output through outdoor testing, and also demonstrating the feasibility of biomimetic flow control as passive enhancement strategy for a small scale wind turbine operating at low wind speed.

2. Methodology

The NACA 4415 airfoil turbine blade is constructed in CATIA V5 software as shown in Figure 1. In this study, the baseline turbine blade that is based on the NACA 4415 airfoil profile has been chosen because of their lift characteristics at low Reynolds numbers and their wide usage in small wind turbine applications. The NACA 4415 profile features a 4% maximum camber located at 40% chord and a 15% maximum thickness, providing a good lift-to-drag ratio across different angles of attack. Both blades have a chord length of 10 cm and a spanwise of 30 cm.

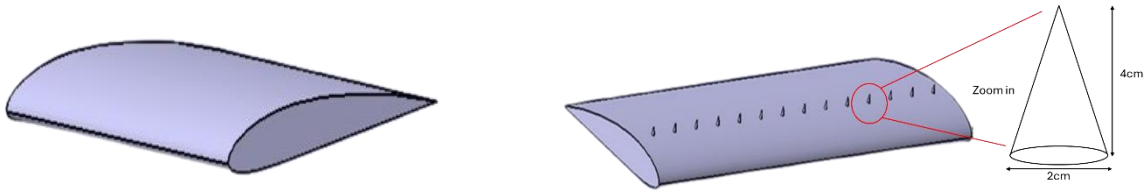

(a) Baseline turbine blade (b) Turbine blade with microspike vortex generator

Figure 1: CAD model of NACA 4415 airfoil turbine blade used in this study

The microspike vortex generators are attached at 30% from the leading edge of the turbine blade. At this location, the boundary layer is transitioning from laminar to turbulent flow, making it optimal for the vortex generator [13]. Studies on dragonfly wings have indicated that microspikes positioned in the forward region between 20% to 40% of the chord are most effective at delaying flow separation by energizing the boundary layer before the adverse pressure gradient. This forward placement allows the generated vortices to propagate downstream and maintain flow attachment over a larger portion of the blade surface, particularly during the high angle of attack characteristics of H-Rotor Darriues VAWT's turbine operation. For this design, the micropike's height is set at 4 mm with circular cross-section of 2 mm diameter. The height-to-chord ratio of 0.04 is selected based on Ref. [13], which demonstrated this scale to correspond to optimal vortex generation without an excessive drag penalty. The microspike vortex generators are arranged in a spanwise spacing that is set at 20 mm, yielding a spacing-to-height

ratio of 5, which ensures adequate vortex interaction while preventing destructive interference between adjacent vortex structures.

For this study, the microspikes are fabricated using Polylactic Acid (PLA) thermoplastic through Fused Deposition Modelling (FDM) 3D printing, integrated directly with the blade structure during additive manufacturing process. Each microspike features a cylindrical geometry with a hemisphere tip to reduce local flow disturbance while maintaining its vortex generation capability. The microspikes are oriented perpendicular to the blade surface, projecting into freestream to maximize interaction with the boundary layer. The fabrication of blades using the 3D printing technique is based on the constructed CAD design models and they are shown in Figure 2. Sandpaper is then used to polish and smoothen the blades' surface in order to reduce skin friction. Next, the blades are painted to reduce skin roughness and have consistent aerodynamic properties.

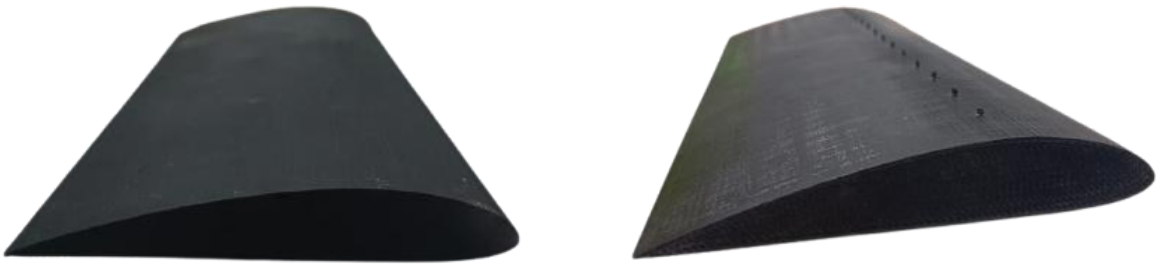

(a) Baseline turbine blade (b) Turbine blade with microspike vortex generator

Figure 2: Fabrication of the NACA 4415 airfoil blades used in this study

The construction of H-Rotor Darrieus VAWT is developed to accommodate both types of blades for analysis (refer Figure 3). The assembly view of the H-Rotor Darrieus VAWT is scaled 1:1 as shown in Figure 3(a). The components used to construct the H-Rotor Darrieus VAWT are (1) blade holder, (2) airfoil blades, (3) cap, (4) copper coil motor, (5) perspex plate, (6) cylindrical shaft pipe, (7) plate copper coil motor and also (8) base frame. The developed H-Rotor Darriues VAWT is shown in Figure 3(b). The base frame is constructed using the wooden stick with dimensions of 150 mm x 150 mm x 150 mm. The blade holder linkage to the cylindrical shaft pipe will rotate the copper coil motor and mechanically generate power output during rotation. The airfoil blade has a sufficient momentum to rotate and spin the cylindrical shaft pipe around to complete one rotation. Data for rotation-per-minute (RPM), wind power, tip speed ratio, torque coefficient and also power output are collected during the experimental testing.

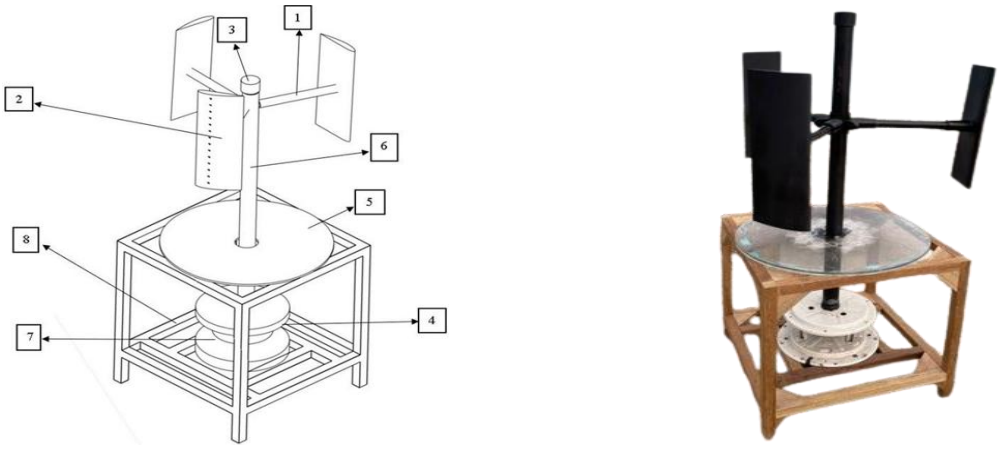

(a) Isometric view in CAD software (b) Developed H-Rotor Darriues VAWT

Figure 3: Construction and development of H-Rotor Darriues VAWT

An analysis of uncertainty has been carried out to measure the error for the experimental testing. The wind speed uncertainty has been found to be between the range of ±0.1 m/s to ±0.19 m/s in the uncontrolled environment. Meanwhile, the rotor blade speed has an uncertainty in the range between ±1.62 rpm to ±4.1 rpm. Moreover, the uncertainty analysis also measures airfoil blade dimensions. The chord length has an uncertainty of ±0.07 cm whereas the spanwise has an uncertainty of ±0.11 cm. Additionally, for the microspike vortex generator, the uncertainty of their height, radius and spacing is ±0.07 cm, ±0.06 cm and ±0.05 cm, respectively.

In this study, experimental investigation is conducted through outdoor testing in an uncontrolled environment to evaluate the real-world performance under natural wind conditions. For the baseline configuration, the H-Rotor Darriues VAWT is installed with the standard NACA 4415 airfoil blades without any surface modifications. The turbine is mounted on the wooden base frame at a height of 30 cm above the ground level to minimize ground interference. The testing site is selected at an open space with minimal obstruction within a radius of 50 m to ensure relatively uniform wind flow. Meanwhile, for the microspike configuration, the same turbine assembly is used with the blades featuring integrated micropsike vortex generators, maintaining the same identical mounting condition and location to ensure fair comparison. Wind velocity measurements are taken using a digital anemometer positioned at the same height as the turbine rotor plane, located 1 m upstream of the turbine to capture the undisturbed wind speed. The anemometer is applied to record instantaneous wind speeds throughout each run test. Rotational speed measurements are obtained using a non-contact optical tachometer that is aimed at a reflective tape marker on the rotating shaft. In addition, power output is measured through the copper coil motor connected to the rotating shaft, whereby the readings of voltage and current are recorded to calculate the electrical power generation.

For each of the blade configurations (baseline and microspike vortex generators), 10 samples' data sets are collected, with each sample set consisting of five simultaneous measurements of wind speed and blade rotation speed taken at 30-second intervals. It should be noted that the testing is conducted during the daylight hours between 10:00 am to 4:00 pm over multiple days in order to capture varying wind conditions representative of the typical operation scenario. Each turbine configuration is tested on separate days to allow for complete setup verification between trials. Using the obtained data from the experiment testing, the values for wind power (P_w), power output (P_{out}), speed ratio (λ), torque (T) and torque coefficient ($C\tau$) can be determined. As indicated by Equation 1 [15], the kinetic energy per unit mass and mass flow rate are multiplied to determine P_w, where ρ is the density of air, A is the swept area and V is the velocity. Furthermore, the H-Rotor Darrieus VAWT in this investigation study has a maximum peak C_P of 0.35 [15], which is used to calculate P_{out} through Equation 2 [15].

$$P_w = \frac{1}{2}\rho A V^3 \tag{1}$$

$$P_{out} = \frac{1}{2}\rho A V^3 C_p \tag{2}$$

On the other hand, the swept area, A is the part where the wind strikes the turbine and causes the rotor to rotate. Equation 3 [15], where D is the diameter of the rotor and H is the rotor height, can be used to get the value of A for the H-Rotor Darrieus VAWT. Conversely, Equation 4 [15] provides the tip speed ratio (λ), where V is the velocity, R is the turbine's rotating part in rpm and ω is the angular

velocity. It can be noted that when the tip speed ratio increases, the performance of the wind turbine is improved due to the increasing rotational rate.

$$A = DH \tag{3}$$

$$\lambda = \frac{\omega R}{V} \tag{4}$$

The revolving shafts transmit most of the mechanical power that has been extracted from the wind speed. This condition is reflected by the presence of torque, T that can be calculated using Equation 5 [15], where ω is the angular velocity in rad/s and P_w is the wind speed mechanical power in Watts. At a distance of rotor radius from the center, the tangential force acting on the rotor blades has the potential to be converted into torque. Equation 6 [15] represents the torque coefficient, C_τ where T is the torque, ϱ is the density of the air, A is the area for H-Rotor Darrieus VAWT and R is the revolving radius of the rotor.

$$T = \frac{P_w}{\omega} \tag{5}$$

$$C_\tau = \frac{T}{\frac{1}{2}\rho A R V^2} \tag{6}$$

The gathered data is from testing that has been conducted outside in an uncontrolled environment. Data for wind speed and blade rotation are collected for 10 samples, each for a sample size of five. The Malaysia's windy climate serves as the basis for the monitoring of the uncontrolled environment. The result from the parameters of the control chart is used to discuss the results that have been required. It should be noted that the control chart analysis is often used to track variables' changes or fluctuations over time. In this case, the upper and lower limits are the parameters of interest. For this study, these metrics are computed for the average wind speed, rotation of rotor, wind power, tip speed ratio, torque coefficient and power output, as well as the range of results. The upper and lower control limits for the mean values are determined using Equation 7 and Equation 8 [16]. On the other hand, the range values for upper and lower control limits are determined using Equation 9 and Equation 10 [16]. In these equations, $\bar{R}$ is the range and $\bar{\bar{X}}$ is the mean value of all subgroups. Additionally, the sample size-based process control chart variables, A_2, D_4 and D_3 are provided in the process control chart factors, which are based on sample size. It is noted that the sample in this study is five and not more than seven, hence LCLR is not included.

$$UCL_X = \bar{\bar{X}} + A_2\bar{R} \tag{7}$$

$$UCL_X = \bar{\bar{X}} - A_2\bar{R} \tag{8}$$

$$UCL_R = D_4\bar{R} \tag{9}$$

$$UCL_R = D_3\bar{R} \tag{10}$$

3. Results and Discussion

The H-Rotor Darrieus VAWT is tested through outdoor testing with a temperature range between 28°C to 32°C in a hot and windy environment. As observed in Figure 4, the average mean value, $\bar{\bar{X}}$ of the wind speed is 4.72 m/s, with upper control limit, UCL_X of 5.6m/s and lower control limit, LCL_X of 3.84 m/s. All the data points fall within the upper and lower control limits, and it shows that the outdoor testing is stable and also well-controlled. The testing setup and blade design are operated without any instability variation. In the meantime, the range chart in Figure 5 indicates the value of the mean range, $\bar{R}$ is 1.53 m/s, with upper control limit, UCL_R of 3.24 m/s and without lower control limit since the sample size is limited to five. For another analysis parameter, the LCL_R is not included. All the ranges demonstrate that both the upper and lower control limits for range value is stable and well-controlled, and no point exceeds the limit lines. The range chart is reliable despite the environmental influences.

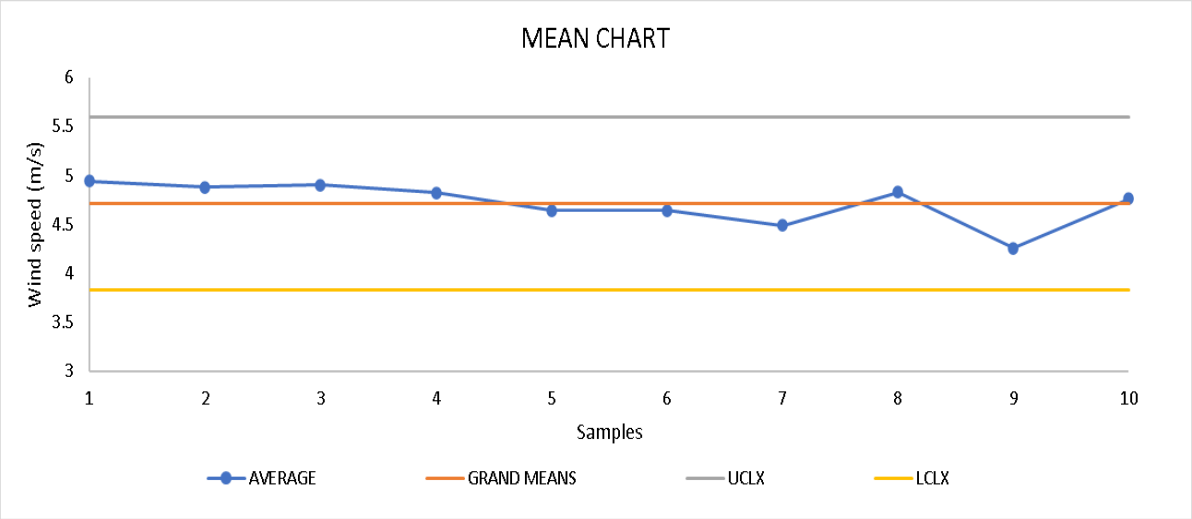

Figure 4: Mean control chart of the wind speed at outdoor testing (uncontrolled environment)

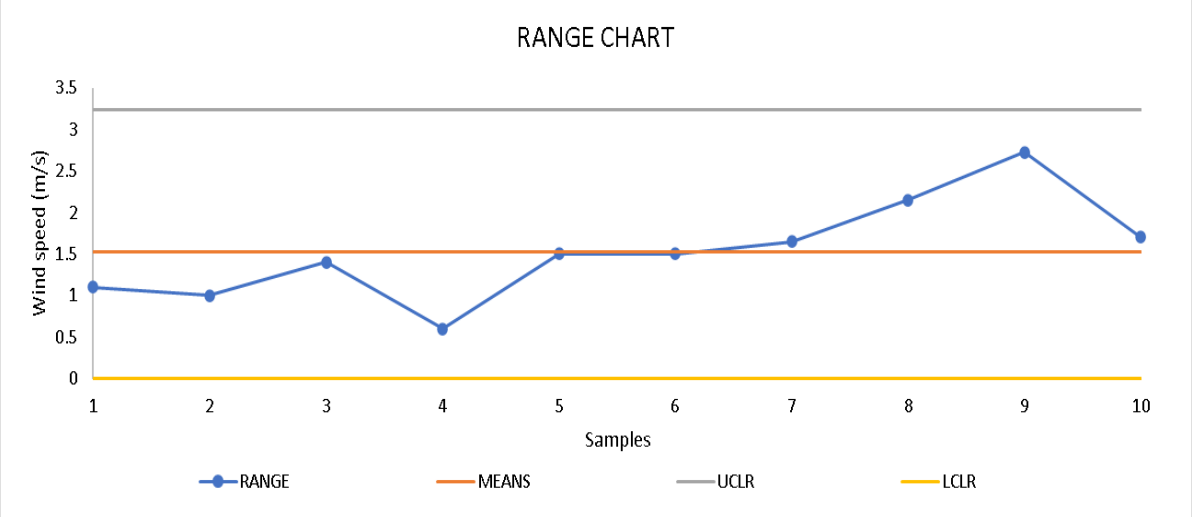

Figure 5: Range control chart of the wind speed at outdoor testing (uncontrolled environment)

Table 1 shows the performance results of the H-Rotor Darrieus VAWT with baseline NACA 4415 airfoil blades and also blades with microspike vortex generators. According to the control chart analysis of both blade rotations, the mean upper control limit and lower control limit have a difference of almost 130 rpm, almost three times for wind power, torque coefficient with 14 times, three times for power output and 11 times for tip speed ratio. Even though the difference between baseline blades and blades with microspike vortex generators is huge, the analysis still shows stability in process control. For the mean upper control limit and range control limit for both blades, the blade rotation obtained 50 RPM difference, almost twice for wind power and power output, 1.7 difference for torque coefficient, and almost a 0.1 difference for tip speed ratio. This indicates that both mean and range control charts show variation but not slight increases.

Table 1: Control Chart analysis for H-Rotor Darrieus VAWT with baseline NACA 4415 blades and NACA 4415 blades with microspike vortex generators

Parameters	Blade rotation (RPM)		Wind power, P_w (Watts)		Torque coefficient, C_τ		Power output, P_{out} (Watts)		Tip speed ratio, λ	
	Base-line	Micro-spike	Base-line	Micro-spike	Base-line	Micro-spike	Base-line	Micro-spike	Base-line	Micro-spike
UCL_X	136.59	151.14	17.61	17.62	7.51	8.98	6.16	6.17	0.38	0.42
Mean	72.79	86.16	12.05	12.11	4.02	4.90	4.22	4.24	0.20	0.24
LCL_X	8.98	21.19	6.50	6.60	0.53	0.82	2.28	2.31	0.02	0.05
Range	110.58	112.61	9.62	9.55	6.05	7.07	3.37	3.34	0.31	0.31
UCL_R	233.77	238.06	20.34	20.19	12.79	14.95	7.12	7.07	0.66	0.68

Figure 6 indicates that the blades with microspike configuration outperform the baseline blades in terms of power generated performance. For the mean value, the blade rotation (RPM) is increased by 18.38%, torque coefficient is increased by 22.01% and also tip speed ratio is increased by 18.71%. This improvement shows that the blades with microspike vortex generator attachments can increase the flow attachment along the blade's surface and decrease drag, which enables the rotor blades to rotate more effectively. There are also slight variations around 0.44% in the power output and wind power, showing better aerodynamic efficiency rather than higher energy consumption. It can be taken that the blades with microspike vortex generator re-energizes the boundary layer and postpones the flow separation, which creates smoother airflow and also increases torque production. The mechanism is synergistically combined to increase the effective lift-to-drag ratio across the operational range of tip speed ratios. The 22% improvement in torque coefficient directly reflects the enhanced tangential force component that is resulting from the maintained lift at higher angles of attack.

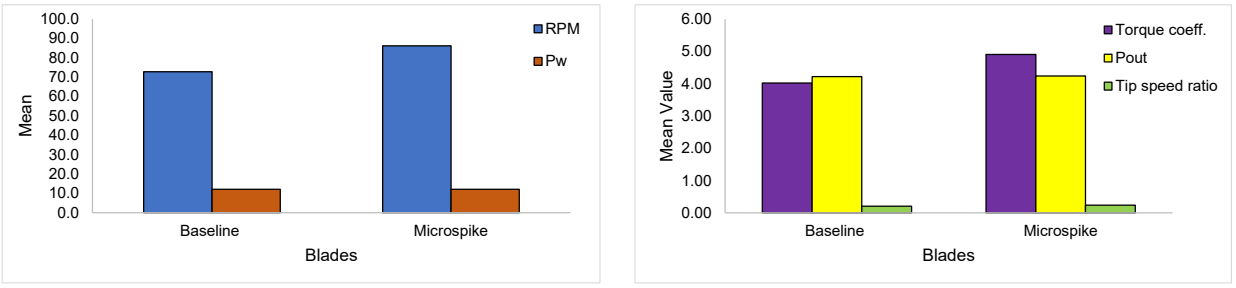

(a) (b)

Figure 6: Comparison of mean value between baseline blades and blades with microspike vortex generator for (a) blade rotation, wind power, (b)torque coefficient, output power and tip speed ratio

On the whole, studies of biomimetic vortex generators modelled after the dragonfly's wing have shown that the microstructures contribute in preserving the steady flow at low Reynolds numbers [13]. With every aspect, the microspike vortex generator adaptation on airfoil blades effectively improves torque production and rotational speed without requiring enormous increase in power. It is also proven that these blades with microspike vortex generators have the potential to reduce aerodynamic drag force and increase the power generated efficiency.

4. Conclusion

Based on mean values from the control chart analysis, the blades with microspike vortex generators have outperformed the baseline blades. The results show that the blade's rotation is increased by almost 18.5%, torque coefficient is increased by 22%, tip speed ratio is increased by 18.7%, and almost 0.5% increment for both wind power and power output. Throughout the test runs, the blades with vortex generators also continuously provide more stable and effective aerodynamic behavior. This microspike vortex generator has the capacity to re-energize the boundary layer and delays the flow separation, thus increasing lift and decreasing drag losses. In terms of power generation, the blades with microspikes vortex generators generate more power on average than the baseline blades. The enhanced performance shows that the enhanced aerodynamic flow structure around the blade's surface led to increased energy with the presence of variable external wind conditions. Blades with microspikes have a stable response during operation as observed by the mean and range control chart analysis. Overall, it can be taken that additional microspike vortex generator on the blades for the H-Rotor Darrieus greatly improves power generation capacity and aerodynamic efficiency in comparison to the baseline blades. This additional biomimetic vortex generator on airfoil blades for H-Rotor Darrieus is also more practical compared to mechanical modification. The controlled environment or indoor testing and parametric optimization studies will be investigated further.

References

[1] A. Eltayesh, F. Castellani, F. Natili, M. Burlando and A. Khedr, 'Aerodynamic Upgrades of a Darrieus Vertical Axis Small Wind Turbine', Energy for Sustainable Development, vol. 73, pp. 126-143, 2023.

[2] M. O. Korukçu, 'Impact of Blade Modifications on the Performance of a Darrieus Wind Turbine', Processes, vol. 12, no. 4, 732, 2024.

[3] K. U. Reddy, B. Deb and B. Roy, 'A Numerical and Experimental Study on the Performance of a Conventional H-Darrieus Wind Rotor with Auxiliary Blades', Ocean Engineering, vol. 280, 114697, 2023.

[4] T. Jiang, Y. Zhao, S. Wang, L. Zhang and G. Li, 'Aerodynamic Characterization of a H-Darrieus Wind Turbine with a Drag-Disturbed Flow Device Installation', Energy, vol. 292, 130522, 2024.

[5] M. Asadbeigi, F. Ghafoorian, M. Mehrpooya, S. Chegini and A. Jarrahian, 'A 3D Study of the Darrieus Wind Turbine with Auxiliary Blades and Economic Analysis based on an Optimal Design from a Parametric Investigation', Sustainability, vol. 15, no. 5, 4684, 2023.

[6] S. H. Rad, F. Ghafoorian, M. Taraghi, M. Moghimi, F. G. Asl and M. Mehrpooya, 'A Systematic Study on the Aerodynamic Performance Enhancement in H-type Darrieus Vertical Axis Wind Turbines using Vortex Cavity Layouts and Deflectors', Physics of Fluids, vol. 36, no. 12, 125170, 2024.

[7] W. Eltayeb, J. Somlal, A. R. Singh and F. Alsaif, 'Enhancing Darrieus Wind Turbine Performance through Varied Plain Flap Configurations for the Solar and Wind Tree', Scientific Reports, vol. 14, no. 1, 30014, 2024.

[8] P. Prakash, P. Laws, S. Mitra and N. Mishra, 'Bioinspired Swept-Curved Blade Design for Performance Enhancement of Darrieus Wind Turbine', Physics of Fluids, vol. 36, no. 8, 085189, 2024.

[9] S. R. Mirmotahari, F. Ghafoorian, M. Mehrpooya, S. H. Rad, M. Taraghi and M. Moghimi, 'A Comprehensive Investigation on Darrieus Vertical Axis Wind Turbine Performance and Self-Starting Capability Improvement by Implementing a Novel Semi-Directional Airfoil Guide Vane and Rotor Solidity', Physics of Fluids, vol. 36, no. 6, 065151, 2024.

[10] W. Chen, T. T. Lam, M. Chang, L. Jin, C. Chueh and G. L. Augusto, 'Optimizing H-Darrieus Wind Turbine Performance with Double-Deflector Design', Energies, vol. 17, no. 2, 503, 2024.

[11] B. Anggara, E. P. Budiana, C. Harsito, K. Enoki, K. Kim, I. Yaningsih and D. D. D. P. Tjahjana, 'Performance Improvement of H-Darrieus Wind Turbine with High Efficiency Vortex Structure Attachment', EVERGREEN, vol. 10, no. 1, pp. 496-503, 2023.

[12] H. Hu and M. Tamai, 'Bioinspired Corrugated Airfoil at Low Reynolds Numbers', Journal of Aircraft, vol. 45, no. 6, pp. 2068-2077, 2008.

[13] Y. Kawamura, H. Naka, Y. Sunami and H. Hashimoto, 'Effects of Micro Spike Structure on Flow around Plate', Presented at 3rd International Conference on Design Engineering and Science, Pilsen, Czech Republic, 2014.

[14] J. Favier, A. Pinelli and U. Piomelli, 'Control of the Separated Flow Around an Airfoil using a Wavy Leading Edge Inspired by Humpback Whale Flippers', Comptes Rendus Mecanique, vol. 340, no. 1-2, pp. 107-114, 2012.

[15] D. Ramirez and A. Rubio-Clemente, 'Design and Numerical Analysis of an Efficient H-Darrieus Vertical-Axis Hydrokinetic Turbine', Journal of Mechanical Engineering and Sciences, vol. 13, no. 4, pp. 6036-6058, 2019.

[16] D. C. Montgomery, Introduction to Statistical Quality Control, John Wiley & Sons Inc., 2013.